Supporting Information

Modulated interfacial electron transfer of MXene-T_x@CoS for oxygen evolution reaction

Xinying Du,[a] Xiaoyun Zhang,[a] Shifan Zhu,[a] Yixue Xu,[a] Yuqiao Wang*[a,b]

a Research Center for Nano Photoelectrochemistry and Devices, School of Chemistry and Chemical Engineering, Southeast University, Nanjing 211189, China

b Yangtze River Delta Carbon Neutrality Strategy Development Institute, Southeast University, Nanjing 210096, China

* Corresponding author. Tel. & Fax +862552090621

E-mail address: yqwang@seu.edu.cn (Y. Wang).

1. DFT Calculations

DFT calculations were performed by using Vienna Ab initio Simulation Package (VASP). The generalized-gradient approximation with Perdew-Burke-Ernzerhof (GGA-PBE) was used for the exchange-correlation interactions. The cutoff energy was set to 500 eV for the plane wave basis. The convergence threshold was conducted as 10^{-6} eV and 0.01 eV $Å^{-1}$ for energy and force, respectively. Monkhorst-Pack grid of 3 × 2 × 1 was used for the DFT calculations.

The four-electron pathway for OER in alkaline can be summarized as follows:

$$* + OH^- \rightarrow *OH + e^- \quad (1)$$

$$*OH + OH^- \rightarrow *O + H_2O(l) + e^- \quad (2)$$

$$* O + OH^- \rightarrow * OOH + e^- \quad (3)$$

$$* OOH + OH^- \rightarrow * + O_2(g) + H_2O(l) + e^- \quad (4)$$

where * meaned the active site on the surface, *OH, *O and *OOH represented the absorbed intermediates of OER.

The change of Gibbs free energy of each OER step (ΔG_i, i = 1,2,3,4) was evaluated by the following equation:

$$\Delta G_i = \Delta E + \Delta ZPE - T\Delta S \quad (5)$$

where ΔE was the change of total energy. ΔZPE and ΔS were the change of the zero-point and entropic contribution, respectively.

The theoretical overpotential η was difined by the equation:

$$\eta = \max \{\Delta G_1, \Delta G_2, \Delta G_3, \Delta G_4\}/e - 1.23V \quad (6)$$

2. Materials characterization

The morphologies and micro-structures of samples were examined by transmission electron microscopy (TEM) and atomic force microscope (AFM, Dimension ICON). TEM, scanning transmission electron microscopy (STEM) and corresponding the energy-dispersive X-ray spectroscopy (EDS) elemental mappings were processed on a FEI Talos microscope with a 200 kV accelerating voltage. The crystalline phase was analysed by X-ray diffraction (XRD, Shimadzu XD-3A) using Cu Kα radiation. X-ray photoelectron spectroscopy (XPS, Kratos AXIS ULTRA) was performed to investigate the valence state of the samples.

3. Results and discussions

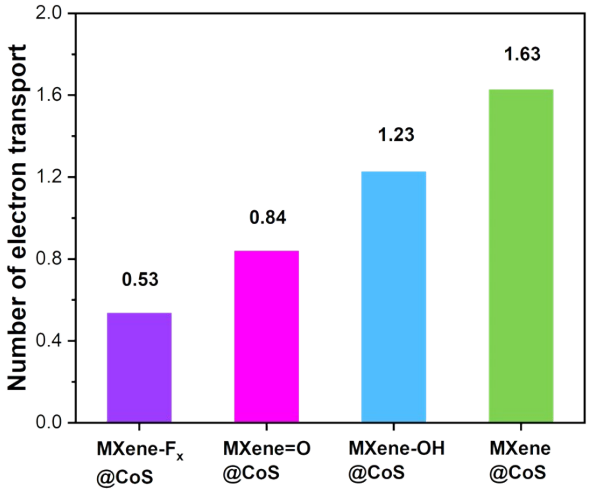

Fig. S1 Interface electron transfer number of MXene-F@CoS, MXene=O@CoS, MXene-OH@CoS and MXene@CoS.

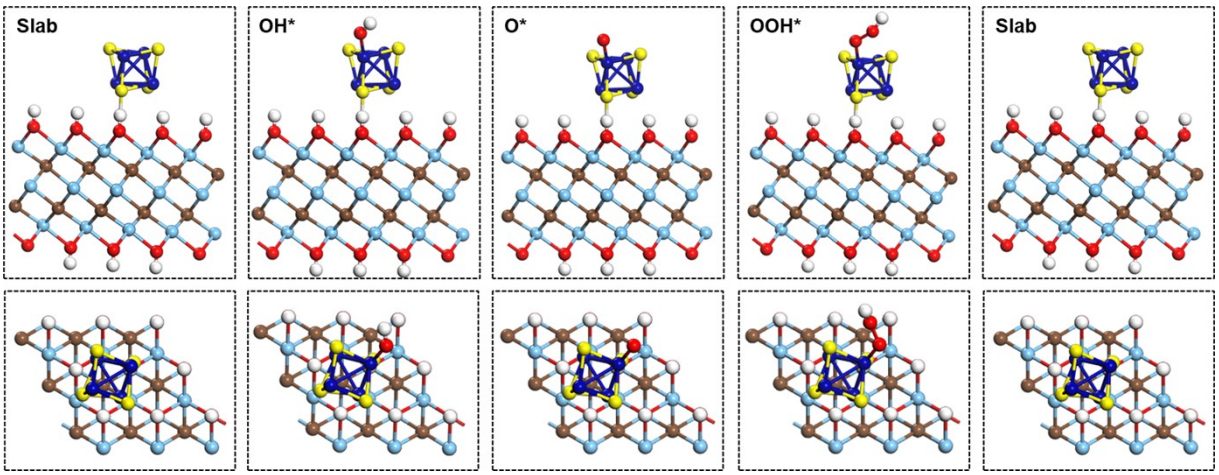

Fig. S2 Adsorption models based on MXene-OH@CoS cell.

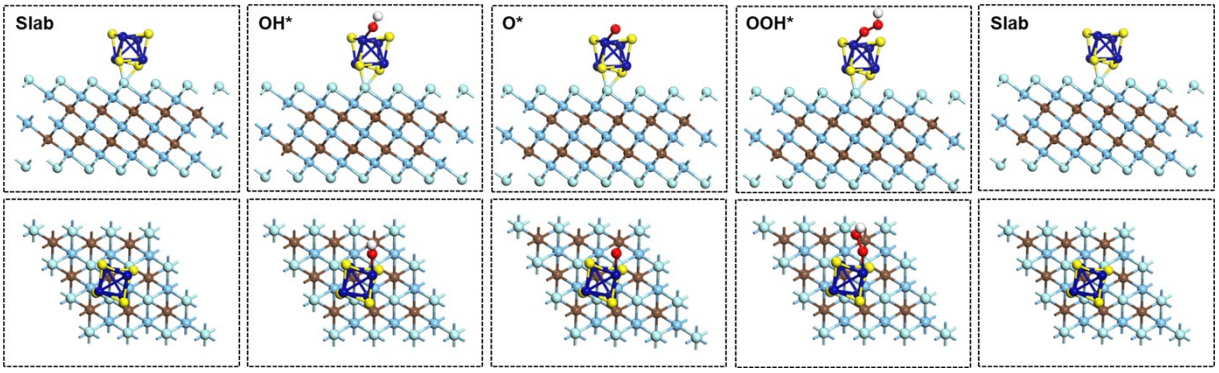

Fig. S3 Adsorption models based on MXene-F@CoS cell.

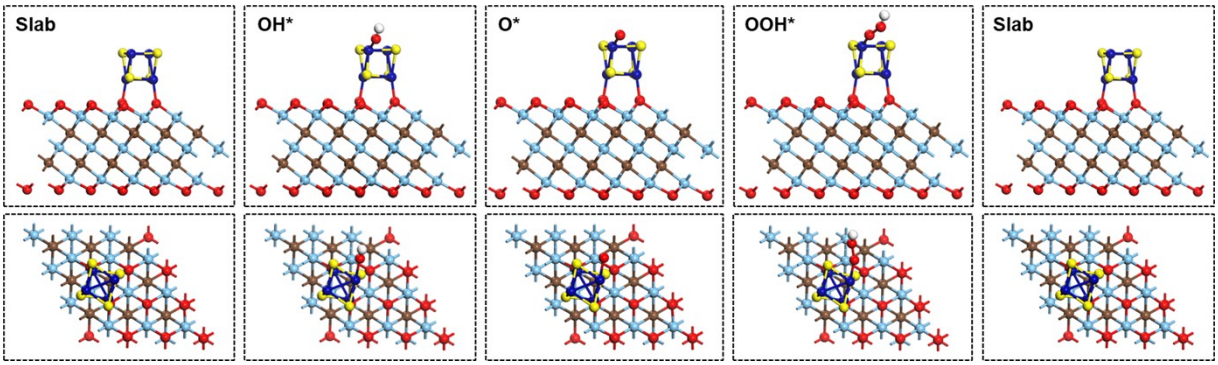

Fig. S4 Adsorption models based on MXene=O@CoS cell.

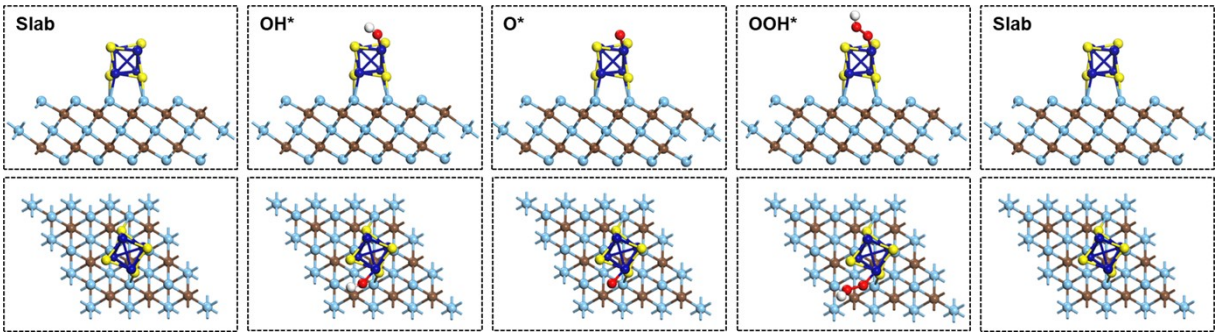

Fig. S5 Adsorption models based on MXene @CoS cell.

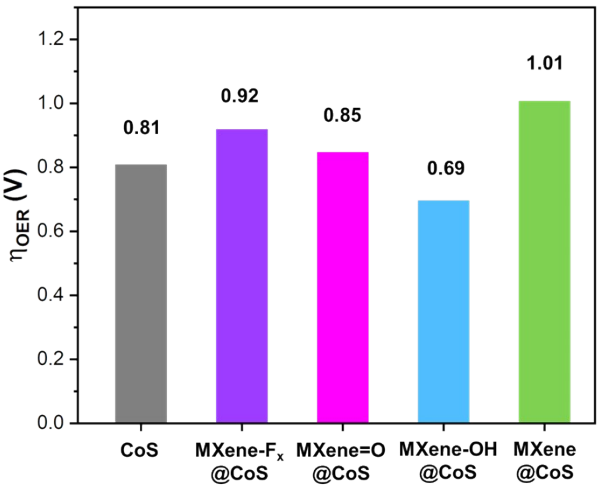

Fig. S6 OER overpotential (η_{OER}) of CoS, MXene-F@CoS, MXene=O@CoS, MXene-OH@CoS and MXene@CoS.

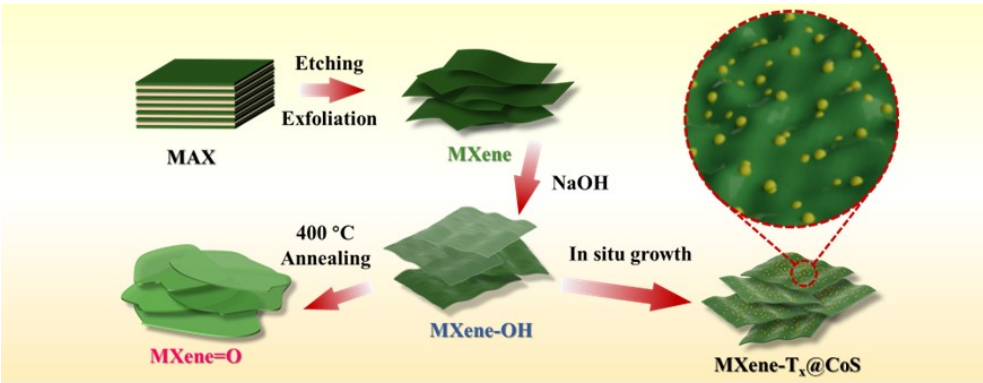

Fig. S7 Schematic illustration of constructing of MXene-T_x@CoS.

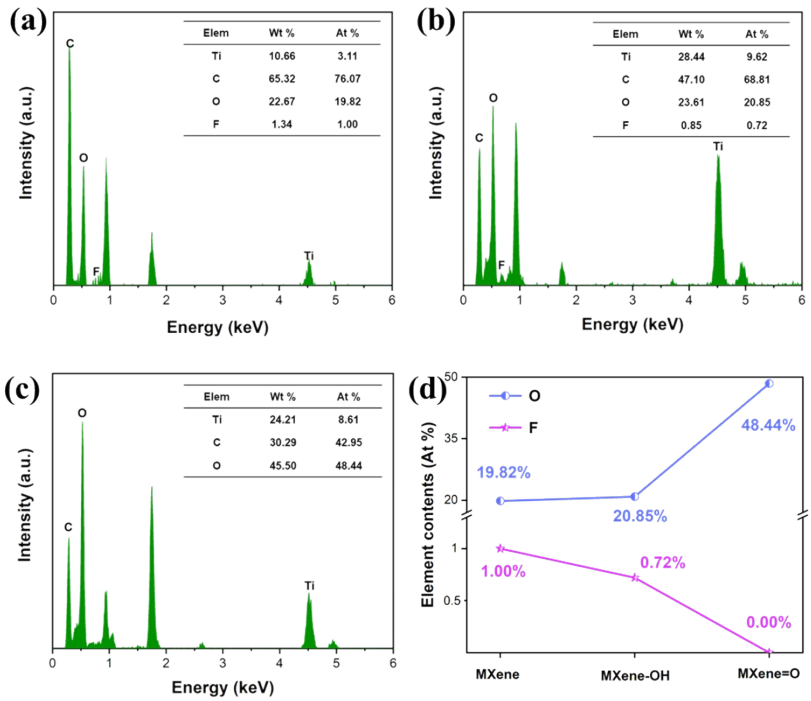

Fig. S8 EDS spectra and the element contents: (a) MXene, (b) MXene-OH and (c) MXene=O, (d) element contents (O and F) of three types of MXene-T_x.

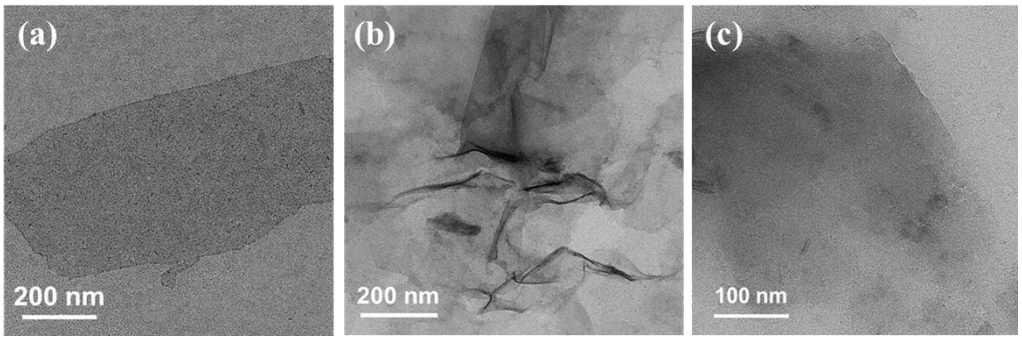

Fig. S9 TEM images of (a) MXene, (b) MXene-OH, and (c) MXene=O.

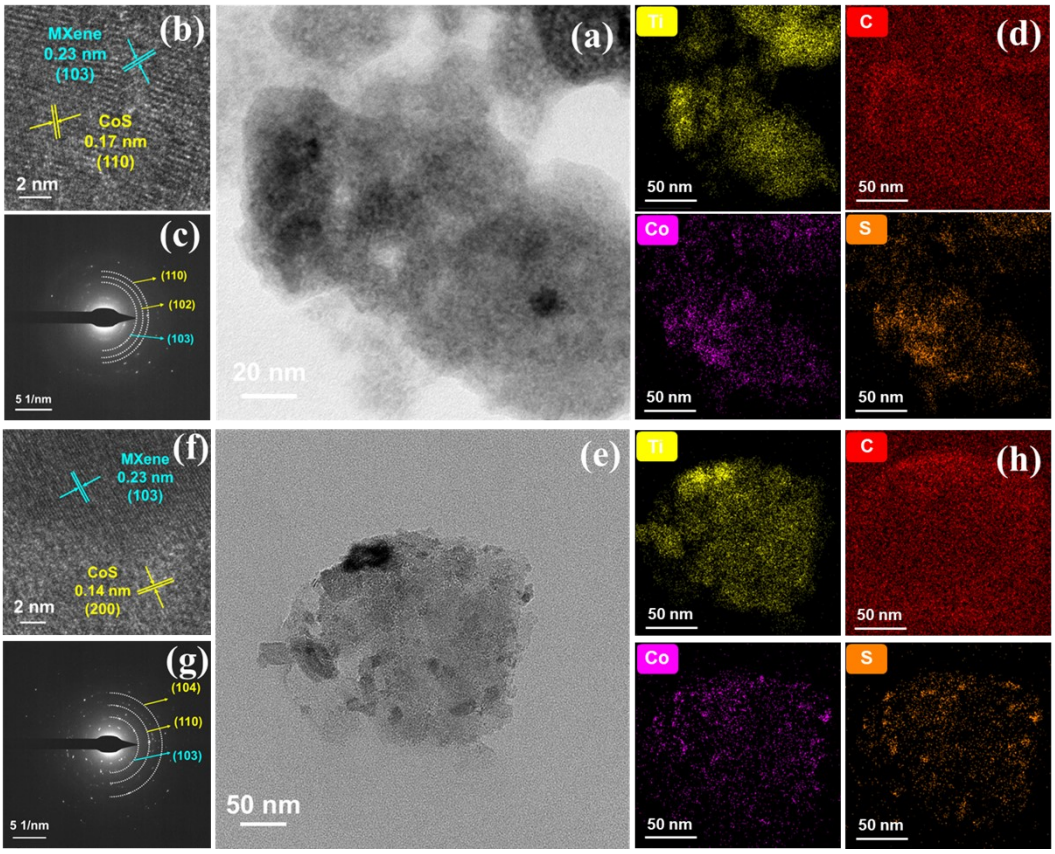

Fig. S10 MXene@CoS: (a) TEM image, (b) HRTEM image, (c) SAED pattern, and (d) elemental mapping images. MXene=O@CoS: (e) TEM image, (f) HRTEM image, (j) SAED pattern, and (h) elemental mapping images.

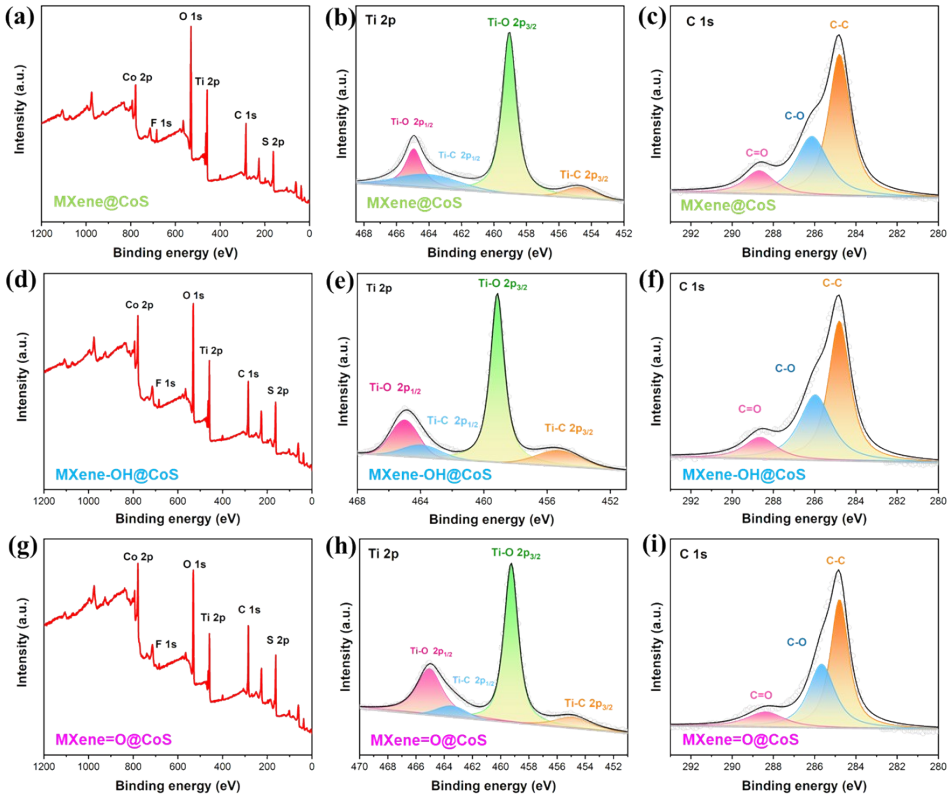

Fig. S11 MXene@CoS: (a) XPS survey curve, spectra of (b) Ti 2p and (c) C 1s; MXene-OH@CoS: (d) XPS survey curve, spectra of (e) Ti 2p and (f) C 1s; MXene=O@CoS: (g) XPS survey curve, spectra of (h) Ti 2p and (i) C 1s.

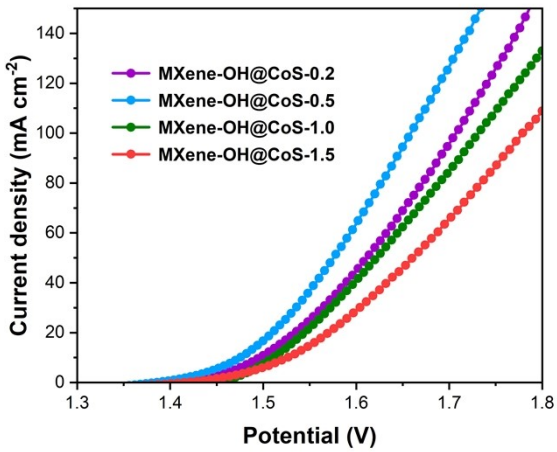

Fig. S12 LSV curves for different contents of CoS in MXene-OH@CoS (0.2, 0.5, 1.0 and 1.5 mmol represent the amount of substance of CoS in 40 mg MXene-OH).

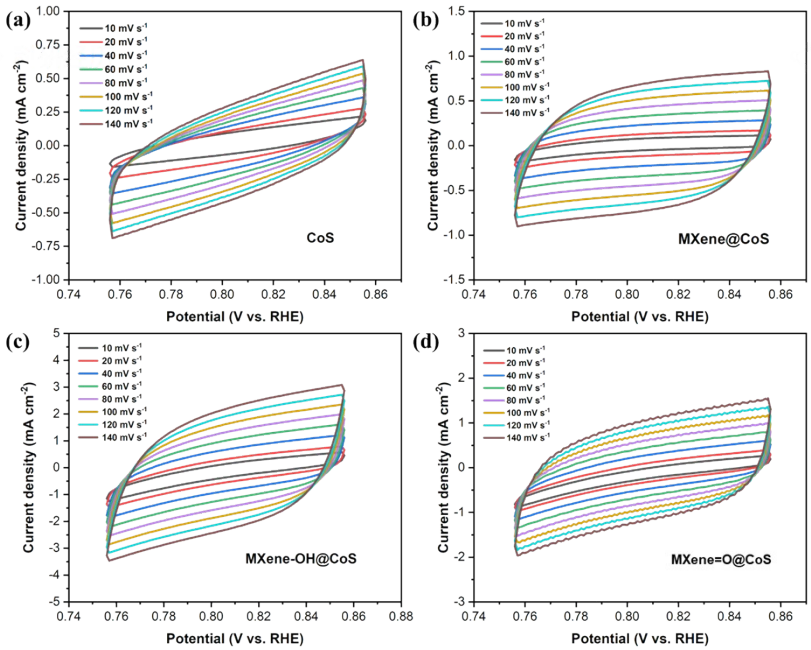

Fig. S13 CV curves of (a) CoS, (b) MXene@CoS, (c) MXene-OH@CoS and (d) MXene=O@CoS.

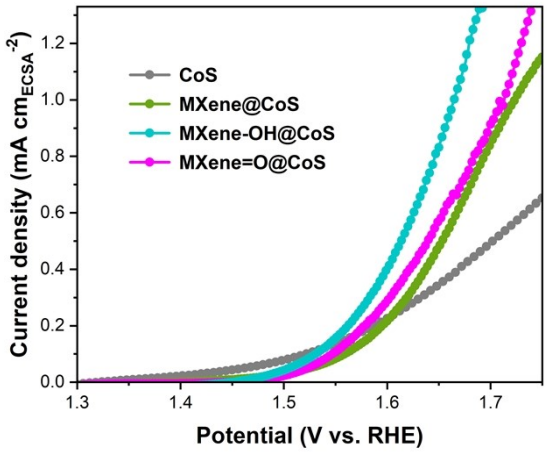

Fig. S14 ECSA-normalized LSV curves of CoS, MXene@CoS, MXene-OH@CoS and MXene=O@CoS.

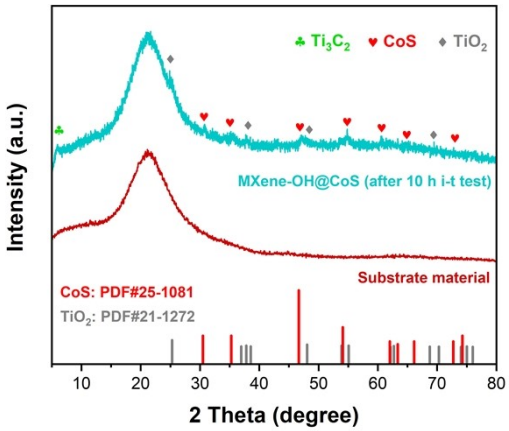

Fig S15 XRD patterns of MXene-OH@CoS after 10 h i-t test.

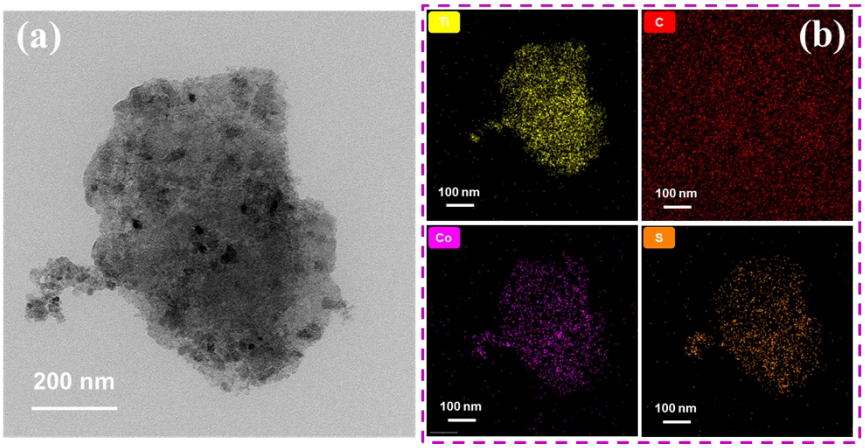

Fig. S16 Images of MXene-OH@CoS after 10 h i-t test: (a) TEM, (b) elemental mapping.

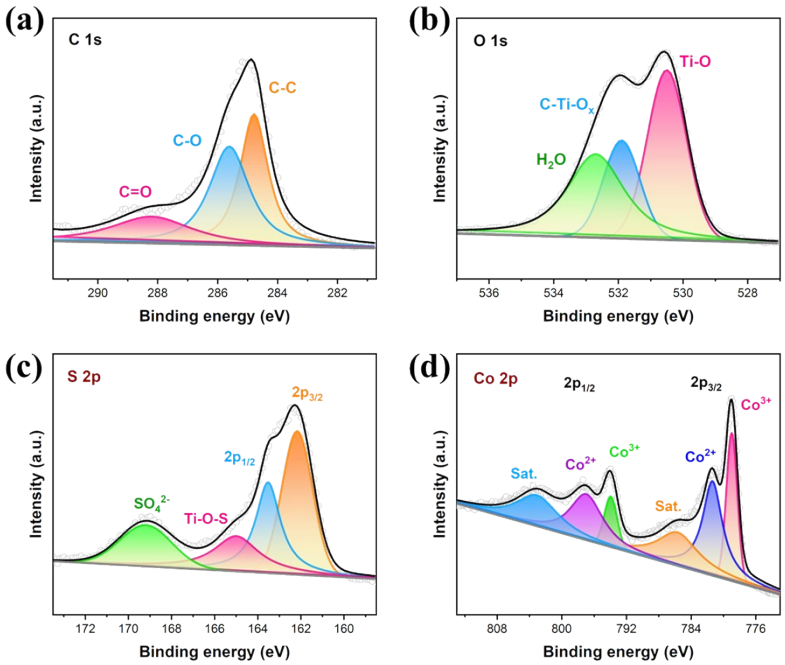

Fig. S17 XPS spectra of MXene-OH@CoS after 10 h i-t test: (a) C 1s, (b) O 1s, (c) S 2p, (d) Co 2p.

Table S1. Calculated values of gibbs free energy on MXene-T_x@CoS slab models.

Intermediates	G (eV) (U = 1.23 V)				
	CoS	MXene-F_x @CoS	MXene=O @CoS	MXene-OH @CoS	MXene @CoS
OH*	-1.23	-0.92	-1.01	-1.28	-1.79
O*	-1.29	-1.11	-1.13	-1.26	-1.97
OOH*	-0.48	-0.19	-0.28	-0.69	-1.01

Table S2 Interplanar spacing of MXene (002), MXene-OH (002), MXene=O (002).

(002)	2θ	d (nm)
MXene	6.30°	1.40
MXene-OH	5.90°	1.50

MXene=O	6.64°	1.33

Table S3 The relative content of Co(III) and Co(II).

Electrocatalyst	Co(III)/Co(II)
CoS	0.80
MXene@CoS	1.24
MXene-OH@CoS	1.27
MXene=O@CoS	1.26

Table S4. Comparisons of OER performance of recently reported catalysts

Electrocatalyst	**OER performance (1M KOH)**		**References**
	η_{10} (mV)	**Tafel slope (mV dec^{-1})**	
MXene-OH@CoS	244	34.9	This work
CoOOH/Co_9S_8	246	86.4	[1]
$Ti_3C_2O_2$@GQDs	250	39.0	[2]
$NiCo_2(OH)_x$/MXene	268	87.0	[3]
CeO_2@CoS/MoS_2	247	64.0	[4]
Co@CoFe–P NBs	266	34.5	[5]
NiFeLa-LDH/v-MXene	255	40.0	[6]
P-CoS_2	250	90.0	[7]
CoP/Mo_2CT_x	260	51.0	[8]
N-CoS_2 YSSs	278	56.0	[9]
$CoFeS_2$/NC	340	56.2	[10]
Fe/Co-CNT@MXene	360	80.0	[11]
CoS/CoO PNRs	265	76.7	[12]

Fe_{MC}–MXene/GrH	296	58.2	[13]
H_2PO^{2-}/FeNi-LDH-V_2C	250	46.5	[14]
NiFeP/MXene	286	35.0	[15]

Table S5. The fitted parameters for the Nyquist plots using the equivalent circuit.

Catalyst	**R_s (Ω)**	**R_1 (Ω)**	**R_2 (Ω)**	**R_{total} (Ω)**
MXene@CoS	2.238	0.5322	2.229	2.761
MXene-OH@CoS	1.605	0.2397	2.161	2.401
MXene=O@CoS	1.607	0.7442	2.363	3.107
CoS	2.277	-	6.749	6.749

References

1 N. Yao, G. Wang, H. Jia, J. Yin, H. Cong, S. Chen and W. Luo, *Angew Chem Int Ed Engl*, 2022, **61**, e202117178.

2 Y. Ma, Y. An, Z. Xu, L. Cheng and W. Yuan, *Science China Materials*, 2022, **65**, 3053-3061.

3 J. Xu, X. Zhong, X. Wu, Y. Wang and S. Feng, *J. Energy Chem.*, 2022, **71**, 129-140.

4 W.-H. Huang, X. M. Li, X. F. Yang, H. Y. Zhang, P. B. Liu, Y. M. Ma and X. Lu, *Chem. Eng. J.*, 2021, **420**.

5 Y. Zhao, N. Dongfang, C. A. Triana, C. Huang, R. Erni, W. Wan, J. Li, D. Stoian, L. Pan, P. Zhang, J. Lan, M. Iannuzzi and G. R. Patzke, *Energy Environ. Sci.*, 2022, **15**, 727-739.

6 M. Yu, J. Zheng and M. Guo, *J. Energy Chem.*, 2022, **70**, 472-479.

7 Y. Li, Z. Mao, Q. Wang, D. Li, R. Wang, B. He, Y. Gong and H. Wang, *Chem. Eng. J.*, 2020, **390**.

8 S. Liu, Z. Lin, R. Wan, Y. Liu, Z. Liu, S. Zhang, X. Zhang, Z. Tang, X. Lu and Y. Tian, *J. Mater. Chem. A*, 2021, **9**, 21259-21269.

9 X. F. Lu, S. L. Zhang, E. Shangguan, P. Zhang, S. Gao and X. W. D. Lou, *Adv.Sci.*, 2020, **7**, 2001178.

10 J. Cai, H. Liu, Y. Luo, Y. Xiong, L. Zhang, S. Wang, K. Xiao and Z. Q. Liu, *J. Energy Chem.*, 2022, **74**, 420-428.

11 C. Zhang, H. Dong, B. Chen, T. Jin, J. Nie and G. Ma, *Carbon*, 2021, **185**, 17-26.

12 Y. Wang, X. Wu, X. Jiang, X. Wu, Y. Tang, D. Sun and G. Fu, *Chem. Eng. J.*, 2022, **434**.

13 T. H. Nguyen, P. K. L. Tran, V. A. Dinh, D. T. Tran, N. H. Kim and J. H. Lee, *Adv. Funct. Mater.*, 2023, **33**, 2210101.

14 Y. Chen, H. Yao, F. Kong, H. Tian, G. Meng, S. Wang, X. Mao, X. Cui, X. Hou and J. Shi, *Appl. Catal. B-Environ.*, 2021, **297**, 120474.

15 J. Chen, Q. Long, K. Xiao, T. Ouyang, N. Li, S. Ye and Z. Q. Liu, *Sci. Bull.*, 2021, **66**, 1063-1072.